Release of a final best-to-use reaction mechanism for syngas combustion modeling

Deliverable 1.1.5

SEVENTH FRAMEWORK PROGRAMME

FP7-ENERGY-2008-TREN-1

ENERGY-2008-6-CLEAN COAL TECHNOLOGIES

Project Acronym: H2-IGCC

Project Full Title: Low Emission Gas Turbine Technology for Hydrogen-rich Syngas

Grant Agreement No.: 239349

SP1: Combustion

Institute of Combustion Technology	Combustion Chemistry Centre	Combustion Technology Group
DLR Stuttgart, Germany	National University of Ireland, Galway	Technical University Eindhoven
Clemens Naumann Jürgen Herzler Peter Griebel	Henry Curran Alan Kéromnès Wayne Metcalfe	Mayuri Goswami

Content

1. Summary

The work of WP1.1 in the subproject SP1 “Combustion” aims at generating a detailed experimental database of the basic combustion properties ignition delay time and laminar flame speed. Detailed kinetic mechanisms for hydrogen and syngas combustion were validated against this experimental data. Ignition delay time data has been measured extensively in a shock tube and a rapid compression machine and a first set of laminar flame data is also available. A comprehensive comparison of experimental results (ignition delay time, laminar flame speed, NO concentration) and simulation results using 5 different detailed mechanisms has been performed in order to suggest a mechanism most suitable for syngas combustion modelling.

The ignition delay time simulations with the mechanisms of NUI Galway [1], Li et al. 2007 [2] and TU/e [4] show a good agreement with the shock tube results for all mixtures, pressures and temperatures. A comparison with literature data and rapid compression machine (RCM) experiments shows that the NUI Galway mechanism is well suited to capture the effect of CO addition.

The results of laminar flame speed simulations using the mechanisms of NUI Galway [1], Li et al. 2007 [2], Li et al. 2011 [3], and TU/e [4] all very similar, only the simulations with the GRI3.0 mechanism [5] show significantly lower flame speed values. The agreement between the simulation results using the mechanisms [1-4] and the measured values is reasonable. This can be attributed to the relatively high uncertainty of the experimental results which poses a high challenge.

All in all, the mechanism of NUI Galway [1] is recommended for hydrogen and syngas combustion because it offers the best level of agreement between experimental data and simulations of combustion properties at all conditions and for all mixtures.

2. Ignition Delay Times

Ignition delay times were measured in a shock tube and in a rapid compression machine (RCM) for a broad variety of operating conditions including gas turbine relevant conditions. Experiments were conducted for different fuel mixtures (H_2, H_2/CO) with and without dilution in the temperature range of 850 - 2375 K, a pressure range of 1 - 32 bar, and different equivalence ratios (Φ = 0.1 – 4.0). The dilution is used for safety reasons in order to limit the heat and pressure release of mixtures with high hydrogen content and it also helps to avoid pre-ignition phenomena. The complementary data sets derived with RCM and shock tube experiments are illustrated in Figure 1 (blue box RCM, red box shock tube).

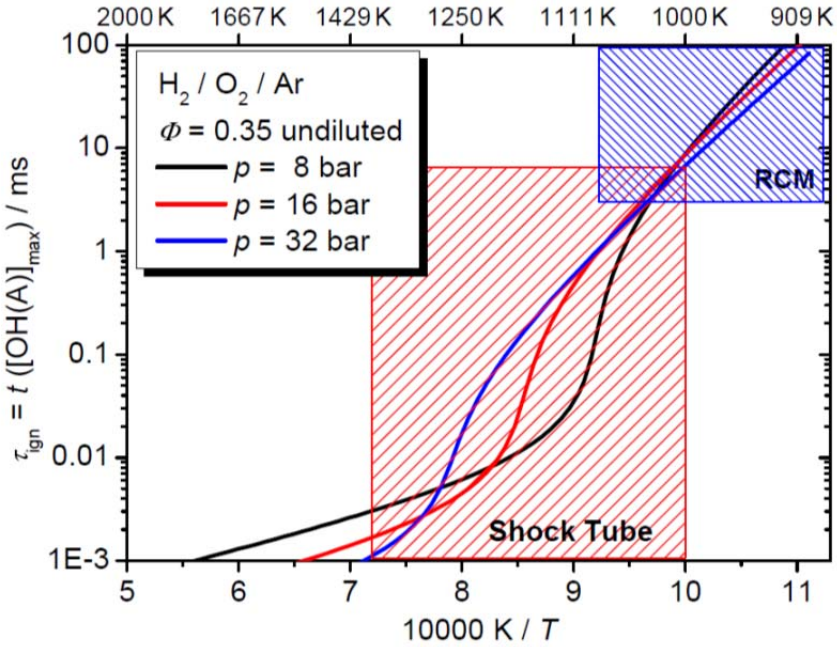

Fig. 1: Complementary temperature regimes of the RCM and shock tube experiments together with simulated ignition delay times for a H_2 / O_2 / Ar (0.7 / 1 / 3.76) mixture using the Li et al. 2007 mechanism [2].

The results of the measurements in the shock tube and the RCM are discussed in detail in the following sections.

2.1 Shock Tube Results (DLR)

The comparison of the experimental results and the simulations using the detailed mechanisms [1-5] are presented in the figures below. The figures 2-7 show ignition delay times of hydrogen, whereas the results of the H2/CO mixtures are shown in the figures 8-13. The operating conditions and the mixtures used for the validation of the mechanisms are listed in Table 1.

Table 1: Fuel mixtures and operating conditions of shock tube (ST) experiments

Case	Fuel	Inert gas	Ø	*P [bar]*	Dilution
ST-1	H_2	Ar	0.1	1, 4, 16	1:5
ST-2	H_2	Ar	0.1	1, 4, 16	undiluted
ST-3	H_2	Ar	0.5	1, 4, 16	1:5
ST-4	H_2	Ar	1	1, 4, 16	1:5
ST-5	H_2	Ar	4	1, 4, 16	1:5
ST-6	H_2	N_2	0.5	1, 4, 16	1:5
ST-7	50 vol% H_2 / 50 vol% CO	Ar	0.5	1, 4, 16	1:5
ST-8	5 vol% H_2 / 95 vol% CO	Ar	0.5	1, 4, 16	1:5
ST-9	50 vol% H_2 / 50 vol% CO	Ar	1.0	1, 4, 16	1:5
ST-10	5 vol% H_2 / 95 vol% CO	Ar	1.0	1, 4, 16	1:5
ST-11	50 vol% H_2 / 50 vol% CO	50 vol% Ar / 50 vol% N_2	0.5	16	1:5
ST-12	85 vol% H_2 / 15 vol% CO	50 vol% Ar / 50 vol% N_2	0.5	16	1:5

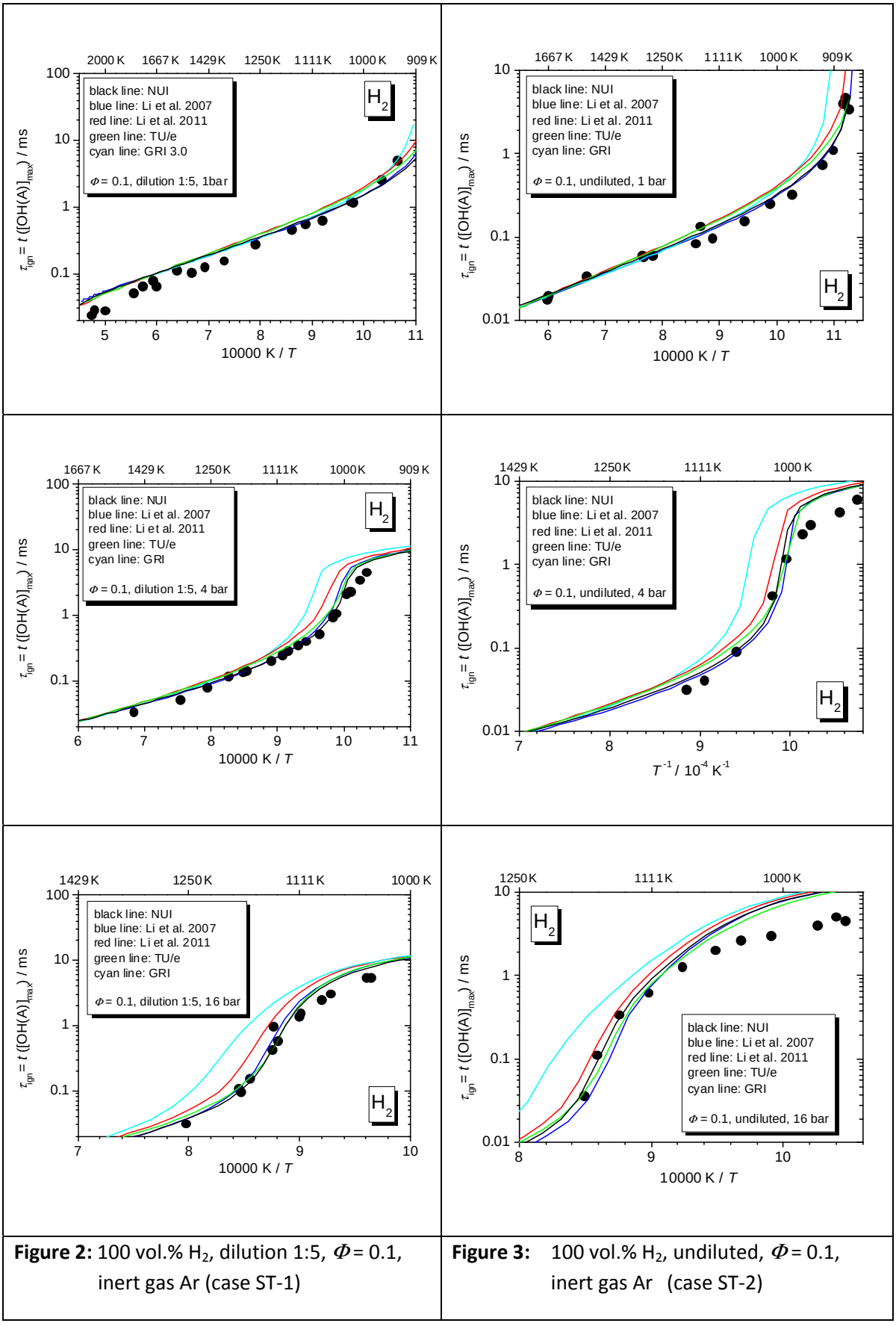

Figure 2: 100 vol.% H_2, dilution 1:5, $\Phi = 0.1$, inert gas Ar (case ST-1)

Figure 3: 100 vol.% H_2, undiluted, $\Phi = 0.1$, inert gas Ar (case ST-2)

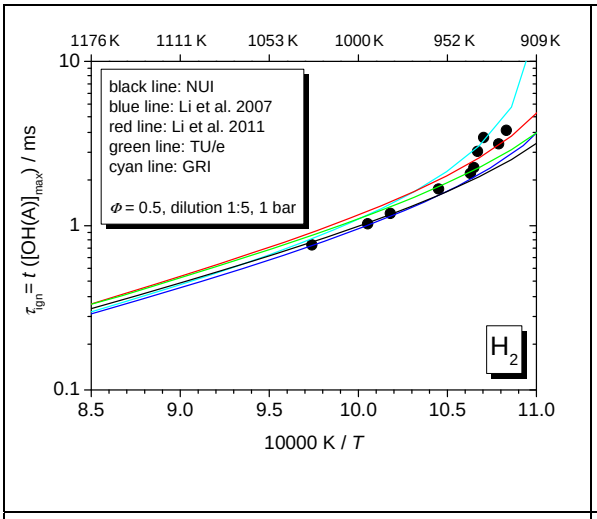

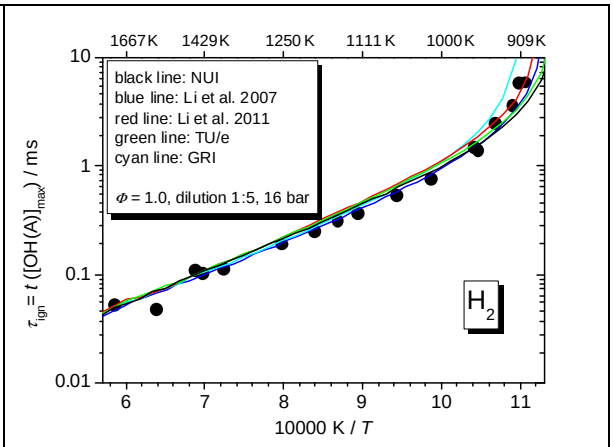

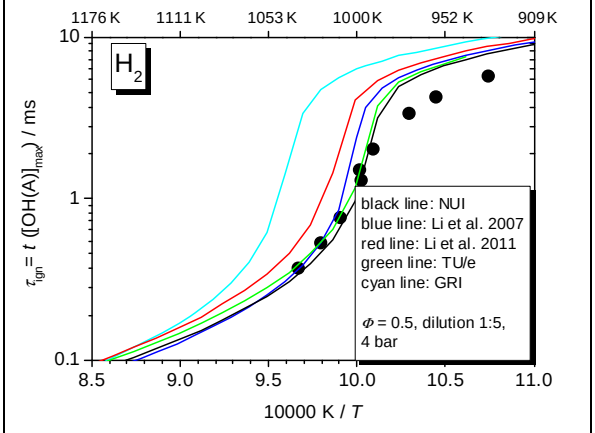

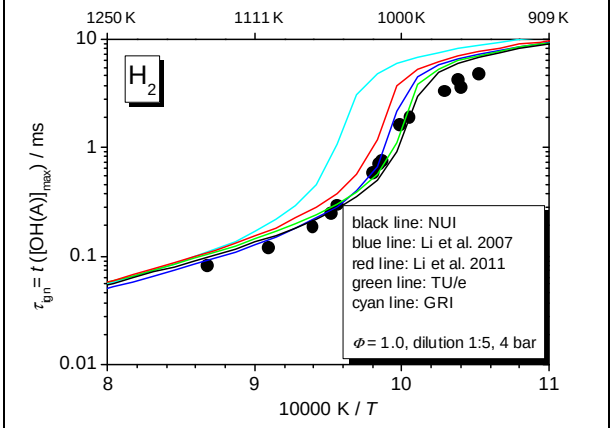

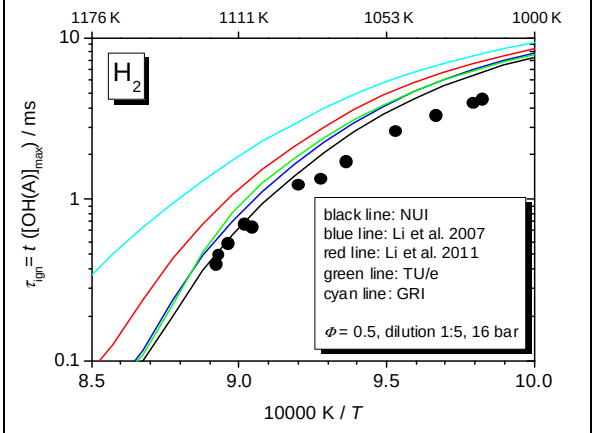

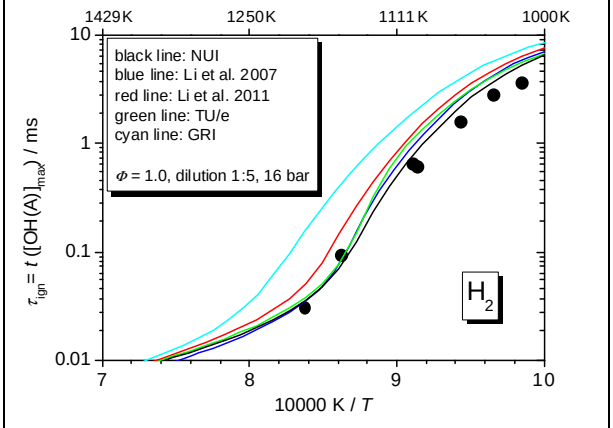

Figure 4: 100 vol.% H_2, dilution 1:5, Φ = 0.5, inert gas Ar (case ST-3)

Figure 5: 100 vol.% H_2, dilution 1:5, Φ = 1.0, inert gas Ar (case ST-4)

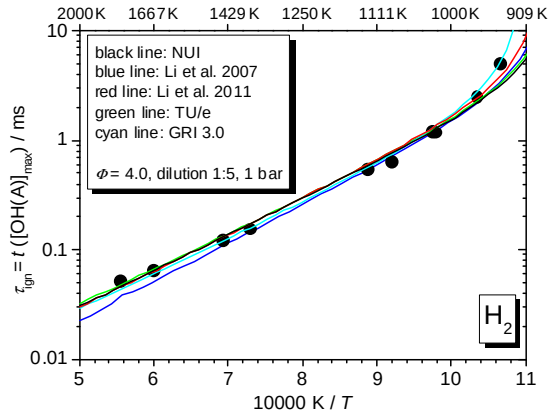

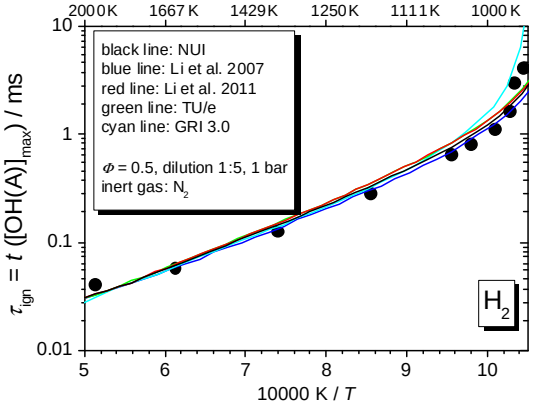

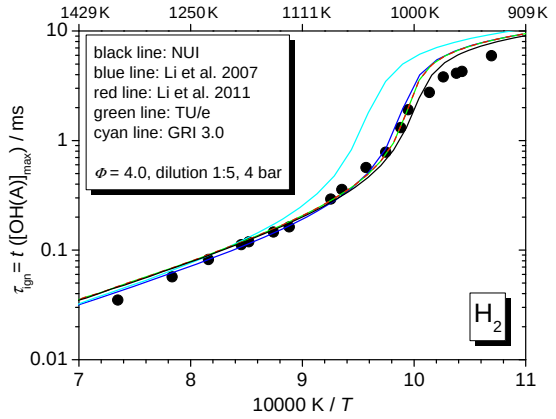

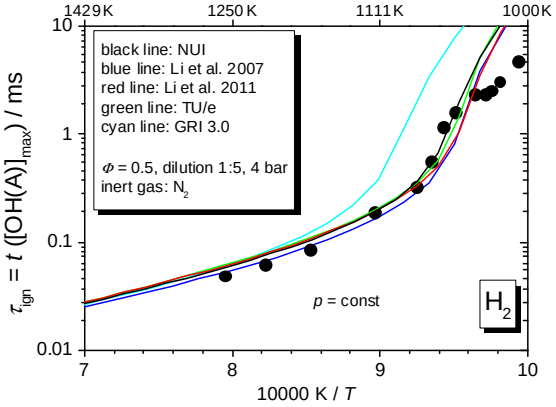

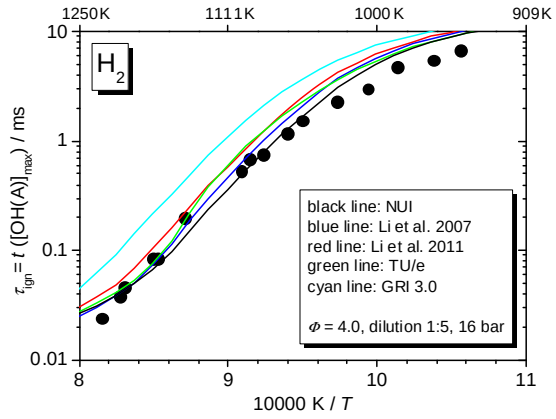

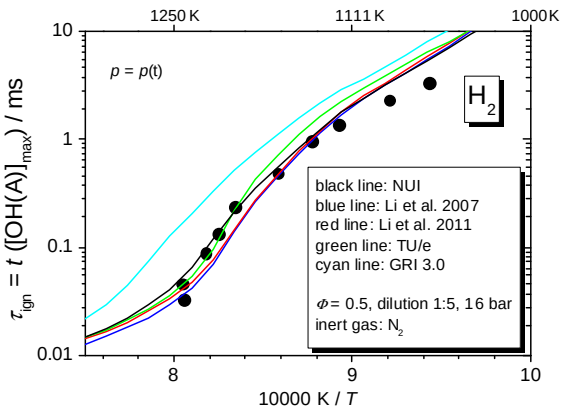

Figure 6: 100 vol.% H_2, dilution 1:5, $\Phi = 4.0$, inert gas Ar (case ST-5)

Figure 7: 100 vol.% H_2, dilution 1:5, $\Phi = 0.5$, inert gas N_2 (case ST-6)

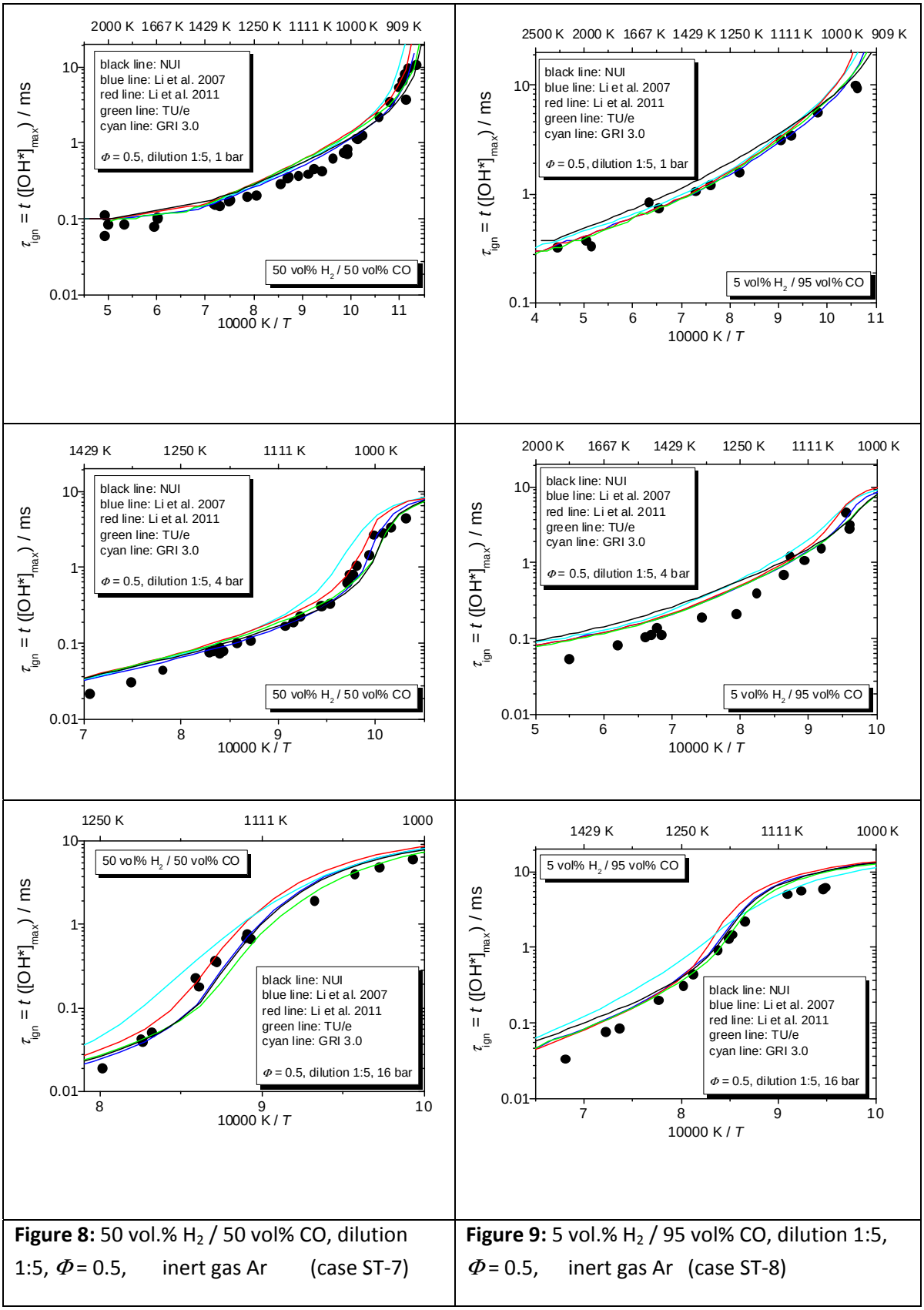

Figure 8: 50 vol.% H_2 / 50 vol% CO, dilution 1:5, $\Phi = 0.5$, inert gas Ar (case ST-7)

Figure 9: 5 vol.% H_2 / 95 vol% CO, dilution 1:5, $\Phi = 0.5$, inert gas Ar (case ST-8)

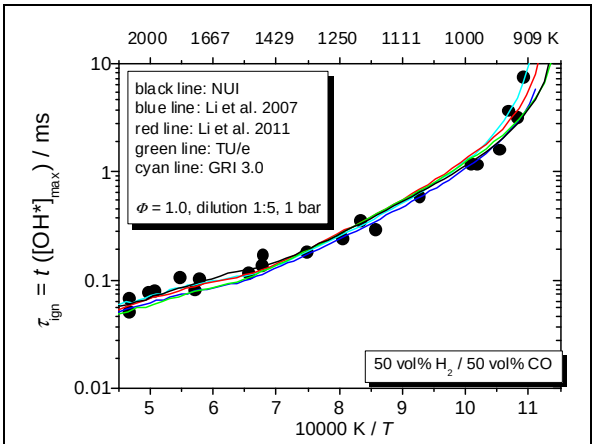

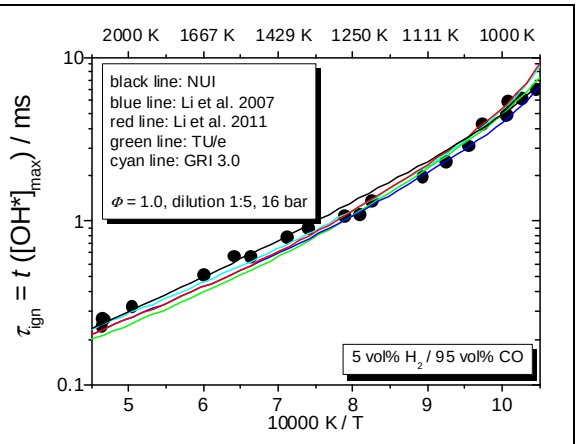

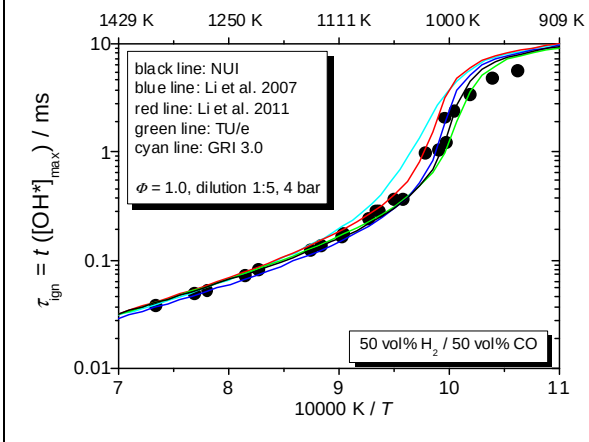

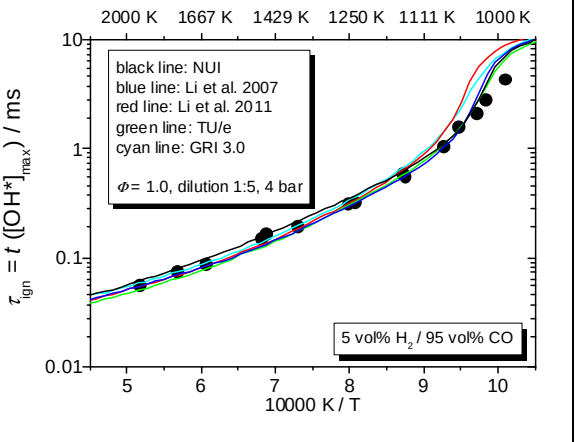

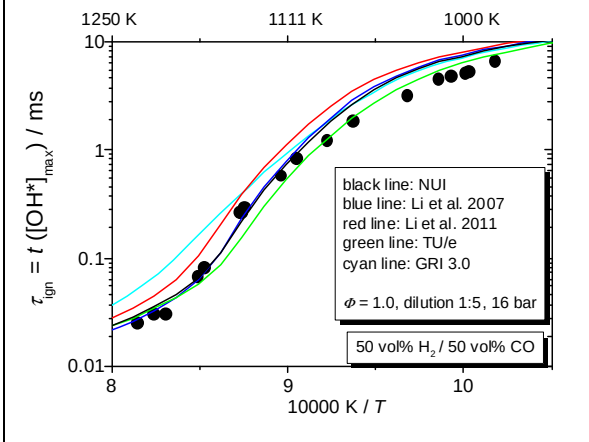

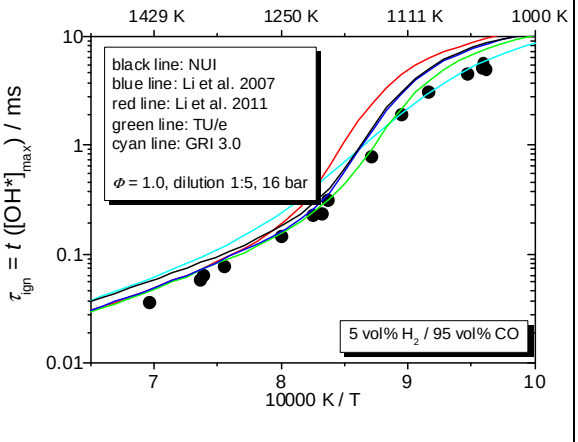

Figure 10: 50 vol.% H_2 / 50 vol% CO, dilution 1:5, Φ = 1.0, inert gas Ar (case ST-9)

Figure 11: 5 vol.% H_2 / 95 vol% CO, dilution 1:5, Φ = 1.0, inert gas Ar (case ST-10)

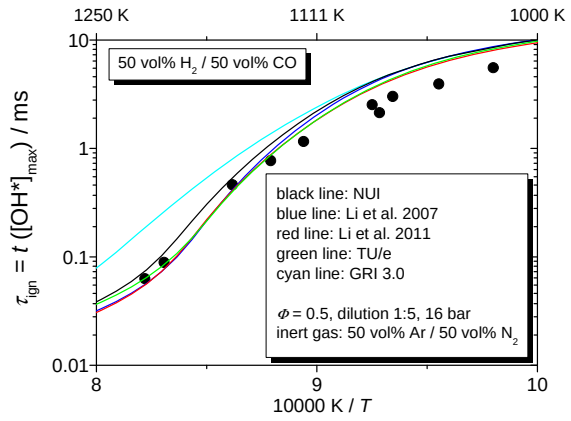

Figure 12: 50 vol.% H_2 / 50 vol% CO, dilution 1:5, Φ = 0.5, inert gas 50 vol% Ar / 50 vol% N_2 (case ST-11)

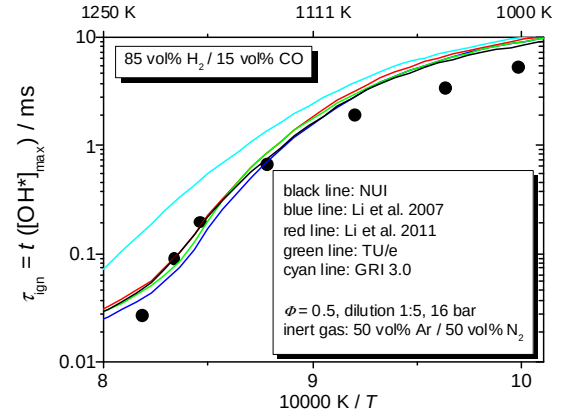

Figure 13: 85 vol.% H_2 / 15 vol% CO, dilution 1:5, Φ = 0.5, inert gas 50 vol% Ar / 50 vol% N_2(case ST-12)

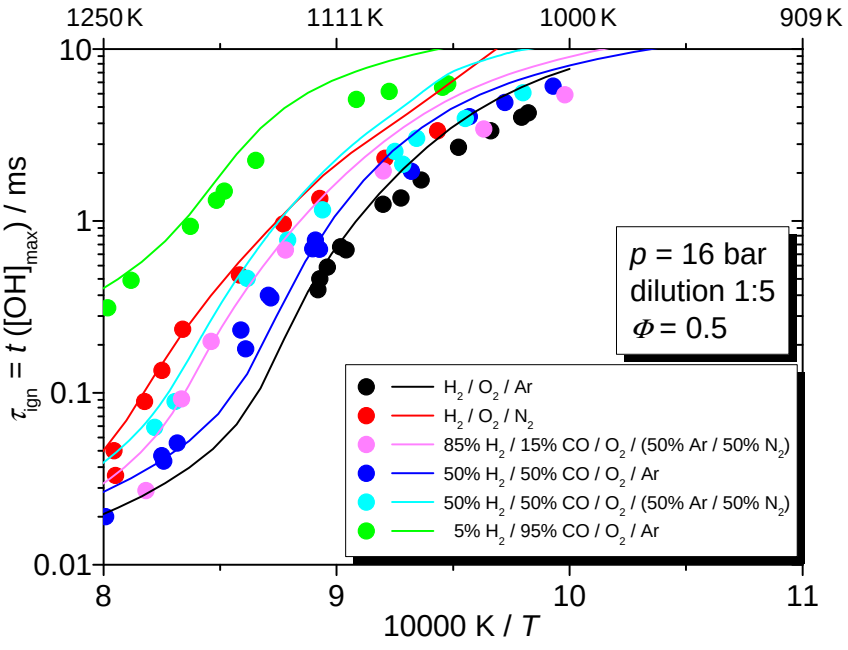

Figure 14: Experiments and simulations with the NUI Galway mechanisms of different H_2 and H_2 / CO mixtures at gas turbine relevant conditions.

Discussion

The simulations with the mechanisms of NUI Galway, TU/e and Li et al. 2007 show a good agreement with the experiments for all mixtures, pressures and temperatures. All mechanisms show a good agreement with the experiments at 1 bar, at higher pressures the GRI3.0 mechanism and the Li et al. 2011 mechanism exhibit too long ignition delay times especially for hydrogen as fuel. The agreement of experiments and simulations at higher pressures using the Li et al. 2011 mechanism is also good for nitrogen or nitrogen/argon mixtures as inert gas.

Figure 14 shows experiments and simulations at gas turbine relevant conditions (16 bar, Ø = 0.5) for different hydrogen and syngas mixtures and different inert gases. The following general characteristics of the hydrogen / syngas system can be seen:

- The influence of CO is quite small for CO concentrations < 20%
- Inert gases with higher collision efficiencies (e.g. N_2 instead of Ar) cause significantly higher ignition delay times.

All these characteristics are very well predicted by the NUI Galway mechanism. The agreement of all presented experiments and simulations is very well for ignition delay times < 1 ms.

At higher ignition delay times the experimental data show shorter values then the predictions. This is probably caused by an insufficient consideration of the gasdynamic temperature increase of the shock tube experiments. In this temperature region even small temperature increases of 10 K cause a decrease of the ignition delay times by 30%.

The values of the 5% H_2 / 95% CO mixture are significantly higher than all other data because of the used definition of the ignition delay time as maximum of the OH* concentration. The fast H_2 oxidation is followed in this mixture by a slow CO oxidation due to the low H_2 content and the dilution. The maximum OH* concentration occurs during the CO oxidation. The good agreement of the measurements and the simulations show that we can not only predict the initiation by the H_2 oxidation but also the slow CO oxidation. The separation of both chemical subsystems was only possible using very high CO concentrations and a dilution of 1:5.

We recommend the mechanism of NUI Galway because it offers the best agreement of experiments and simulations at all conditions especially for hydrogen as fuel. The validation of the mechanisms with respect to shock tube ignition delay times is thus finished.

2.2 Rapid Compression Machine RCM Results (NUI Galway)

Mixtures studied in the NUIG RCM used for mechanism validation are listed in Table 1.

Table 1: Experimental conditions studied in the NUIG RCM

Case	Fuel	Mixture Composition	ϕ	*p* [bar]
RCM-1	H_2	0.7 H_2, 1.0 O_2, 1.881 N_2, 1.881 Ar	0.35	8, 16, 32
RCM-2	H_2	1.0 H_2, 1.0 O_2, 1.881 N_2, 1.881 Ar	0.50	8, 16, 32
RCM-3	85% H_2 15% CO	0.595 H_2, 0.105 CO, 1.0 O_2, 1.881 N_2, 1.881 Ar	0.35	8, 16, 32
RCM-4	85% H_2 15% CO	0.850 H_2, 0.150 CO, 1.0 O_2, 1.881 N_2, 1.881 Ar	0.50	8, 16, 32
RCM-5	50% H_2 50% CO	0.350 H_2, 0.350 CO, 1.0 O_2, 1.881 N_2, 1.881 Ar	0.35	8, 16, 32
RCM-6	50% H_2 50% CO	0.500 H_2, 0.500 CO, 1.0 O_2, 1.881 N_2, 1.881 Ar	0.50	8, 16, 32
RCM-7	25% H_2 75% CO	0.175 H_2, 0.525 CO, 1.0 O_2, 1.881 N_2, 1.881 Ar	0.35	8, 16, 32
RCM-8	25% H_2 75% CO	0.250 H_2, 0.750 CO, 1.0 O_2, 1.881 N_2, 1.881 Ar	0.50	8, 16, 32
RCM-9	5% H_2 95% CO	0.035 H_2, 0.665 CO, 1.0 O_2, 1.881 N_2, 1.881 Ar	0.35	8, 16, 32
RCM-10	5% H_2 95% CO	0.050 H_2, 0.950 CO, 1.0 O_2, 1.881 N_2, 1.881 Ar	0.50	8, 16, 32

As additional RCM validation targets, the models have also been tested against existing data in the literature obtained by Mittal and Sung, with conditions summarised in Table 2.

Table 2: Experimental conditions from Mittal and Sung (Int. J. Chem. Kinet. 38: 516–529, 2006)

Fuel	Mixture Composition	ϕ	*p* bar
H_2	12.5 H_2, 6.25 O_2, 18.125 N_2, 63.125 Ar	1.0	15, 30, 50
75% H_2 25% CO	9.375 H_2, 3.125 CO, 6.25 O_2, 18.125 N_2, 63.125 Ar	1.0	15, 30, 50
50% H_2 50% CO	6.25 H_2, 6.25 CO, 6.25 O_2, 18.125 N_2, 63.125 Ar	1.0	15, 30, 50
35% H_2 65% CO	4.375 H_2, 8.125 CO, 6.25 O_2, 18.125 N_2, 63.125 Ar	1.0	15, 30, 50
20% H_2 80% CO	2.5 H_2, 10.0 CO, 6.25 O_2, 18.125 N_2, 63.125 Ar	1.0	15, 30, 50

The experimental results were compared to the predictions of five different mechanisms [1-5]. The results of the experiments and simulations are presented in the figures below.

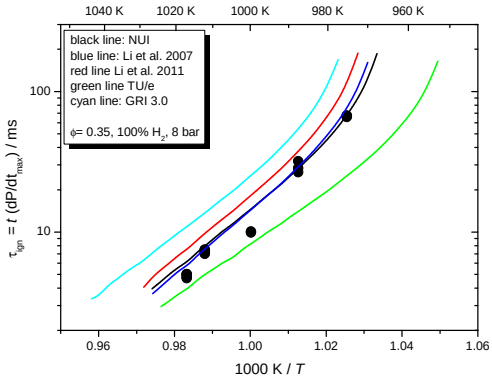

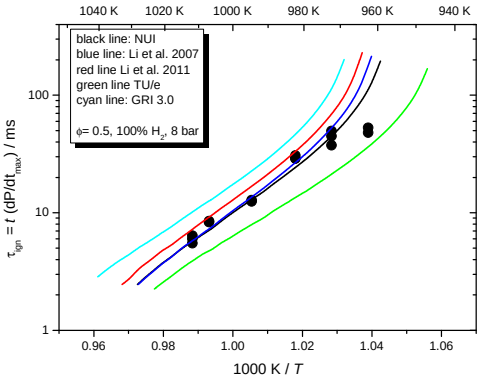

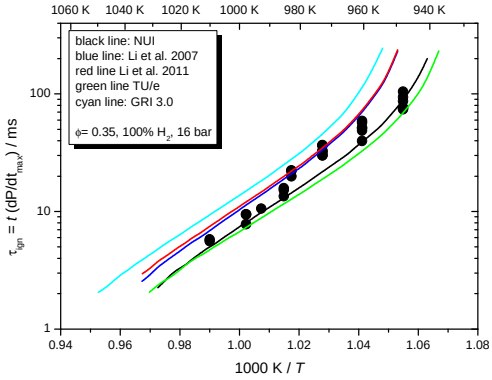

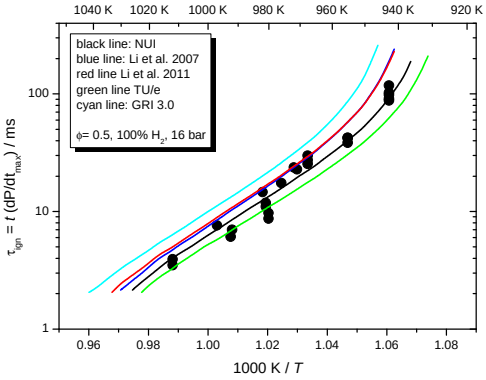

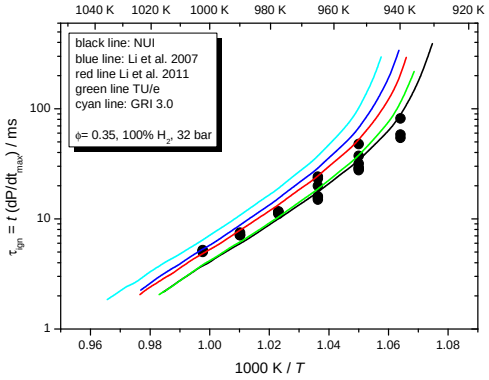

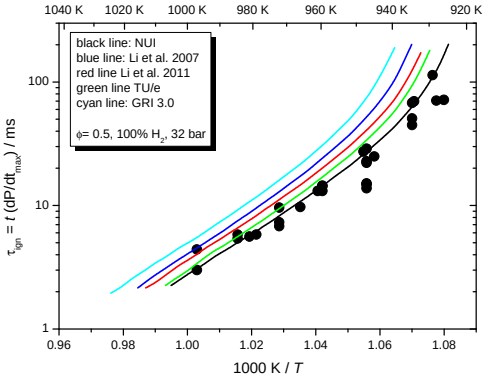

Figure 1: 100% H_2, ϕ = 0.35

Figure 2: 100% H_2, ϕ = 0.50

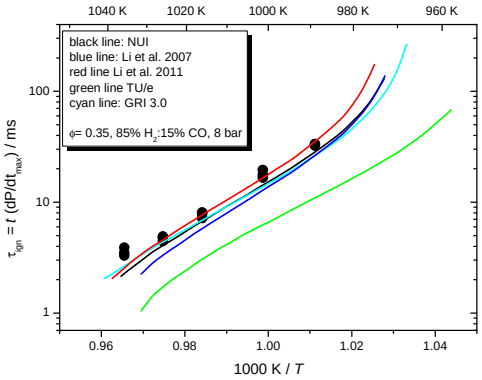

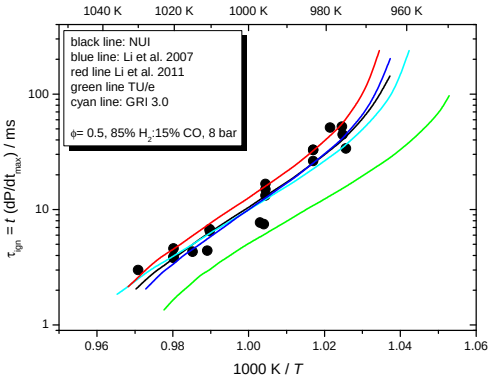

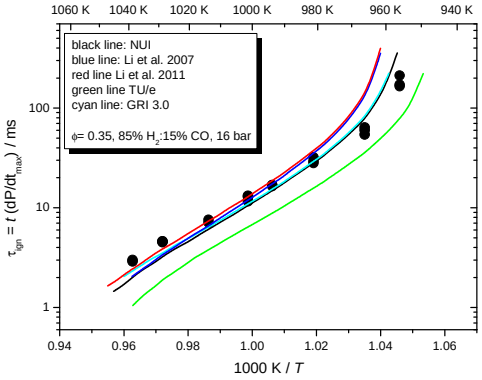

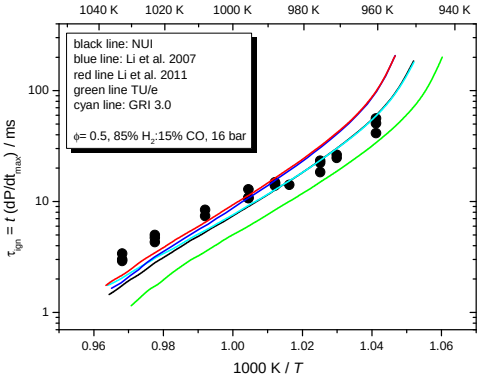

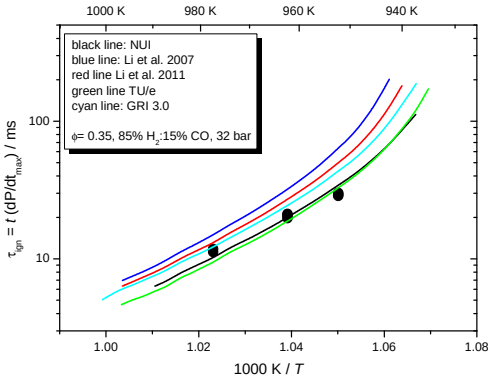

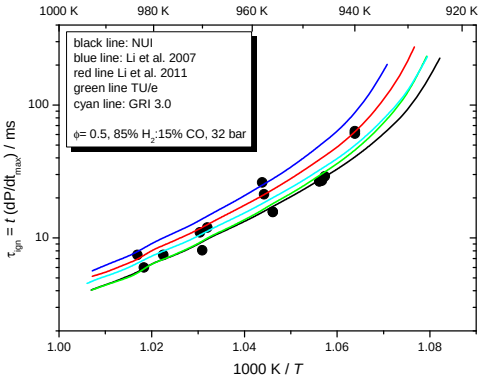

Figure 3: 85% H_2, 15% CO, ϕ = 0.35

Figure 4: 85% H_2, 15% CO, ϕ = 0.50

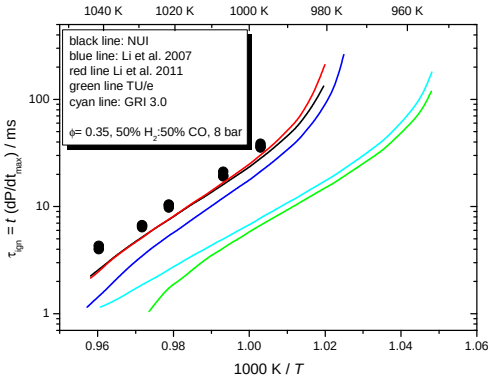

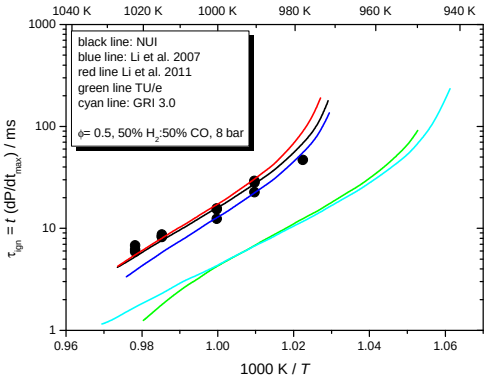

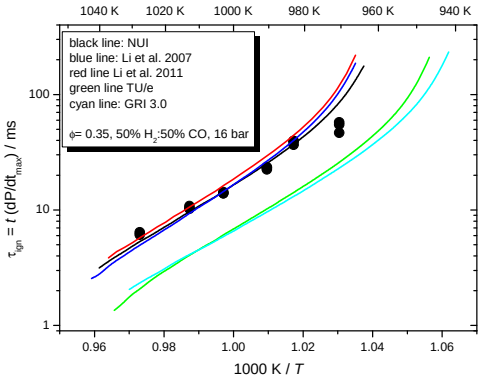

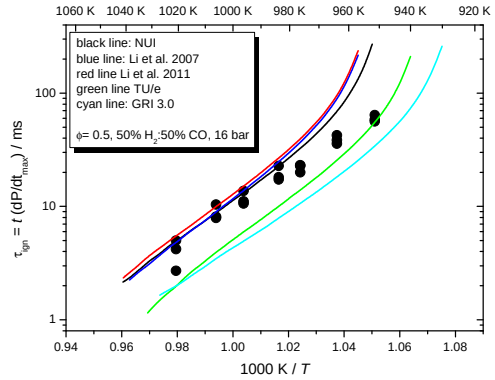

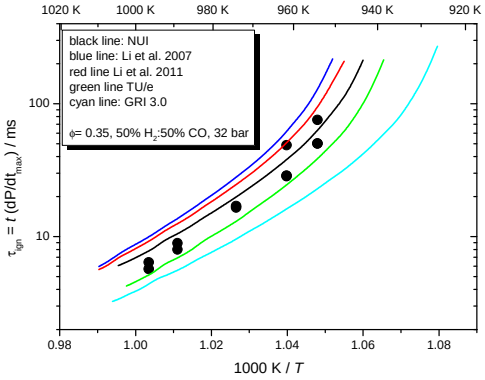

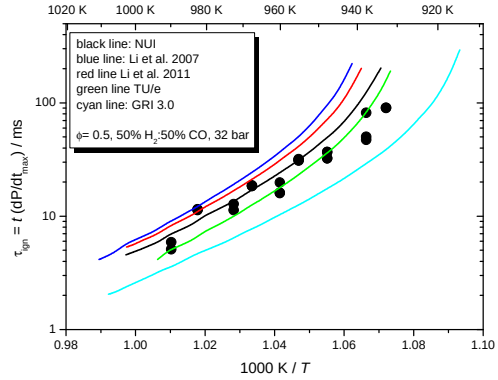

Figure 5: 50% H_2, 50% CO, ϕ = 0.35

Figure 6: 50% H_2, 50% CO, ϕ = 0.50

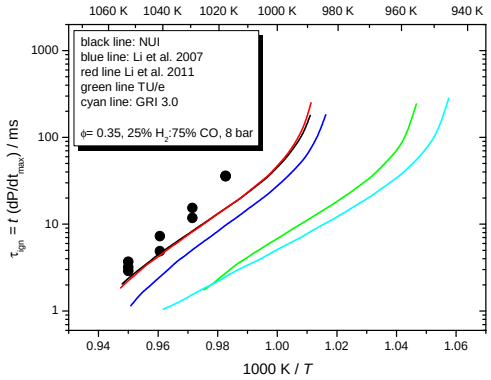

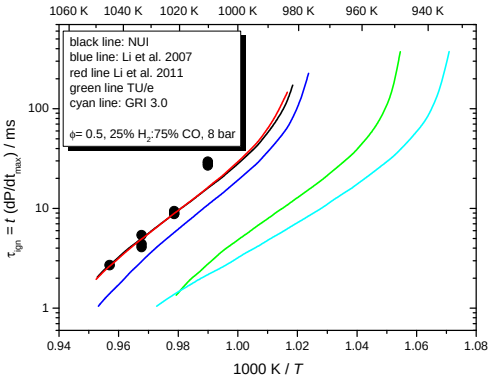

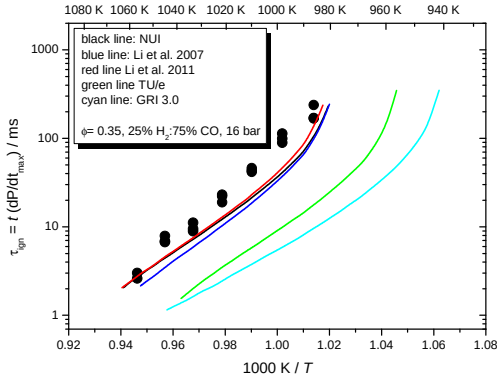

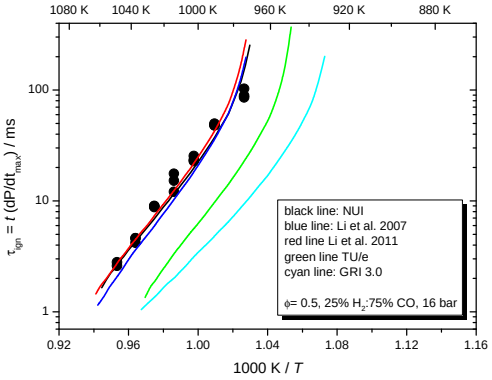

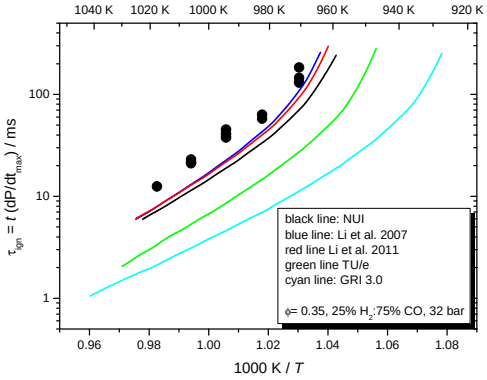

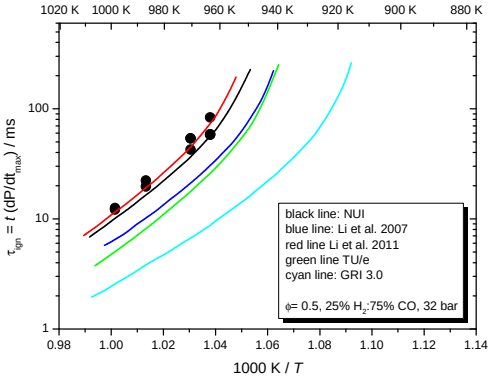

Figure 7: 25% H_2, 75% CO, ϕ = 0.35

Figure 8: 25% H_2, 75% CO, ϕ = 0.50

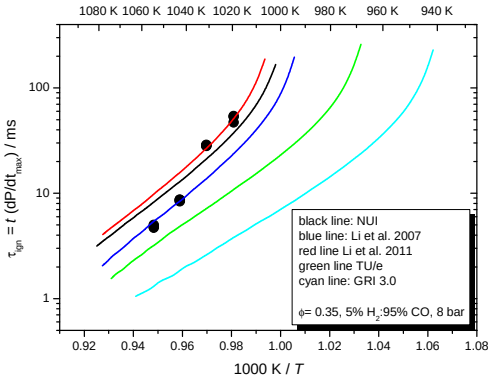

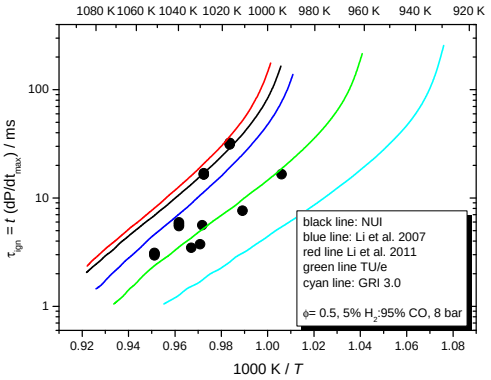

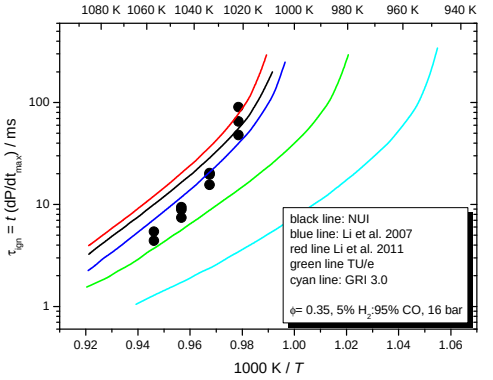

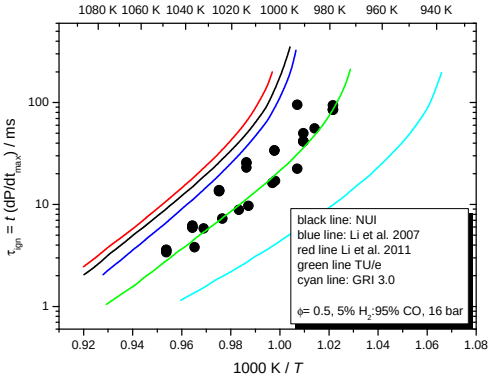

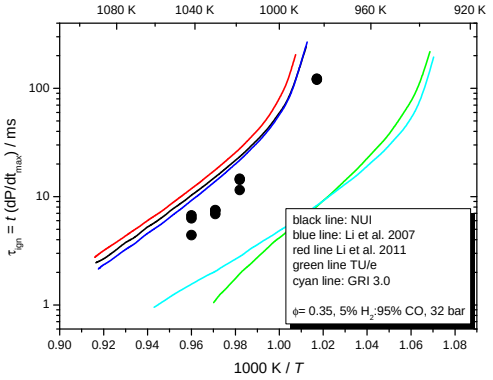

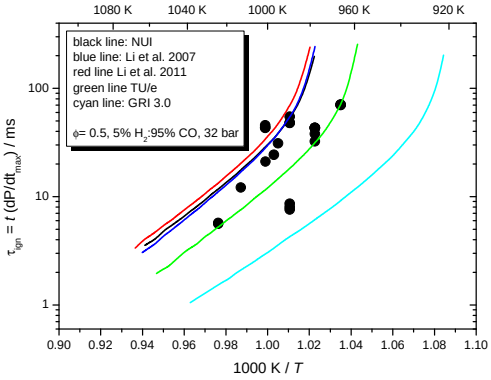

Figure 9: 5% H_2, 95% CO, ϕ = 0.35

Figure 10: 5% H_2, 95% CO, ϕ = 0.50

Mittal and Sung RCM Results

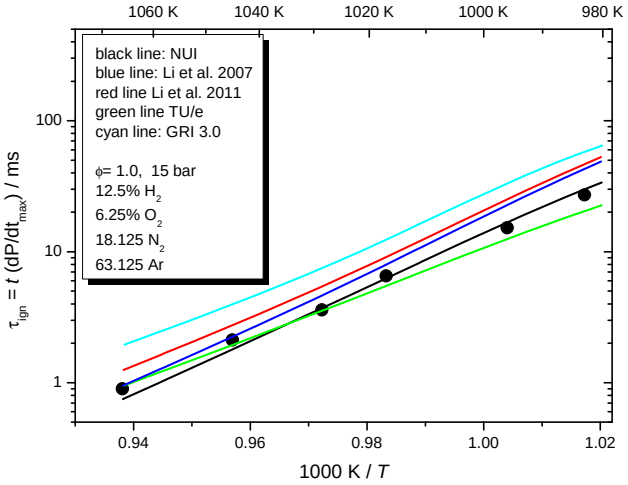

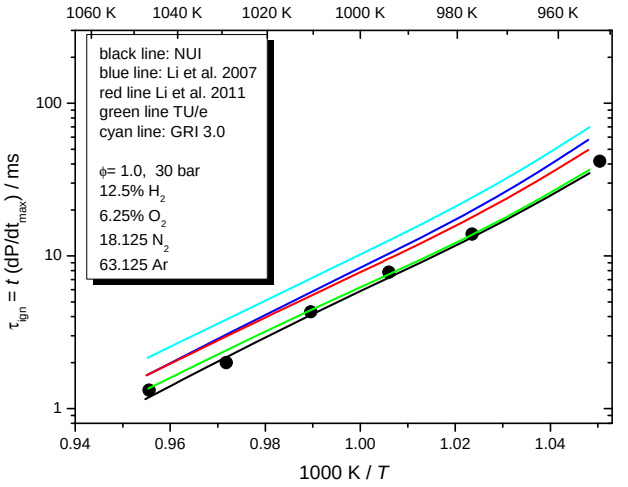

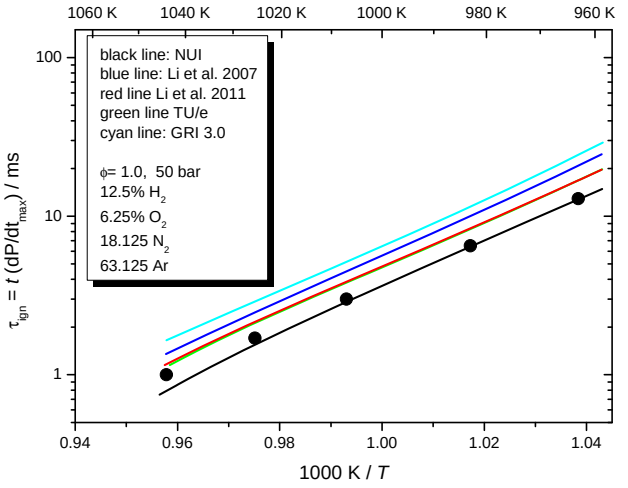

Figure 11: 100% H_2, ϕ =1.0

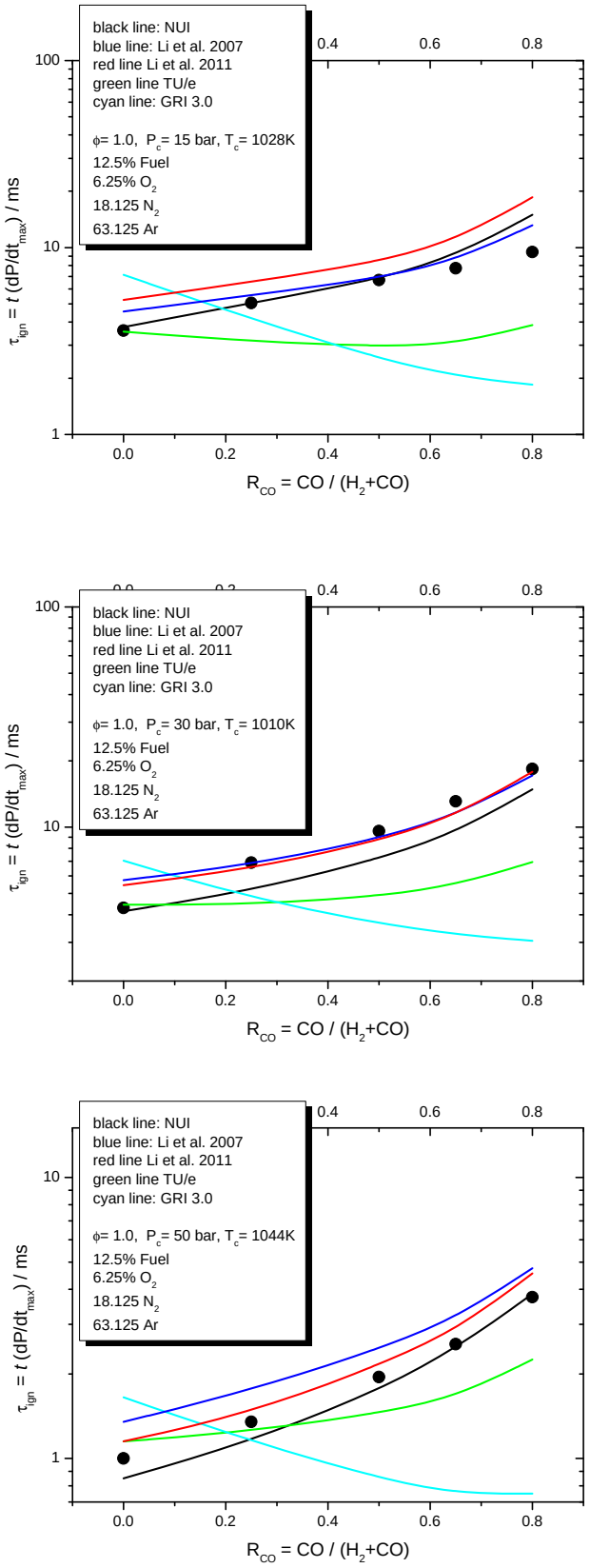

Figure 12: Ignition delay times as a function of CO concentration, $\phi = 1.0$

Recommendation

Overall, the NUIG mechanism performs the best when compared against the NUIG RCM ignition delay data and the existing data from Mittal and Sung. It accurately captures the effect of temperature, pressure and carbon monoxide concentration and is thus recommended for future use in the project.

3. Laminar Flame Speeds (TU/e)

Results of laminar flame speed measurements from literature and performed at TU\e have been compared to simulations using mechanism from NUI (Galway) [1], Li (2007) [2], Li (2011) [3], and TU Eindhoven [4] and GRI 3.0 [5]. The simulations were performed using an in-house one-dimensional laminar flame code CHEM1D [6].

3.1 Comparison with results from Literature

Figures 1-6 show results of the comparison for hydrogen and in Figure 7 an example of a H_2/CO mixture is presented.

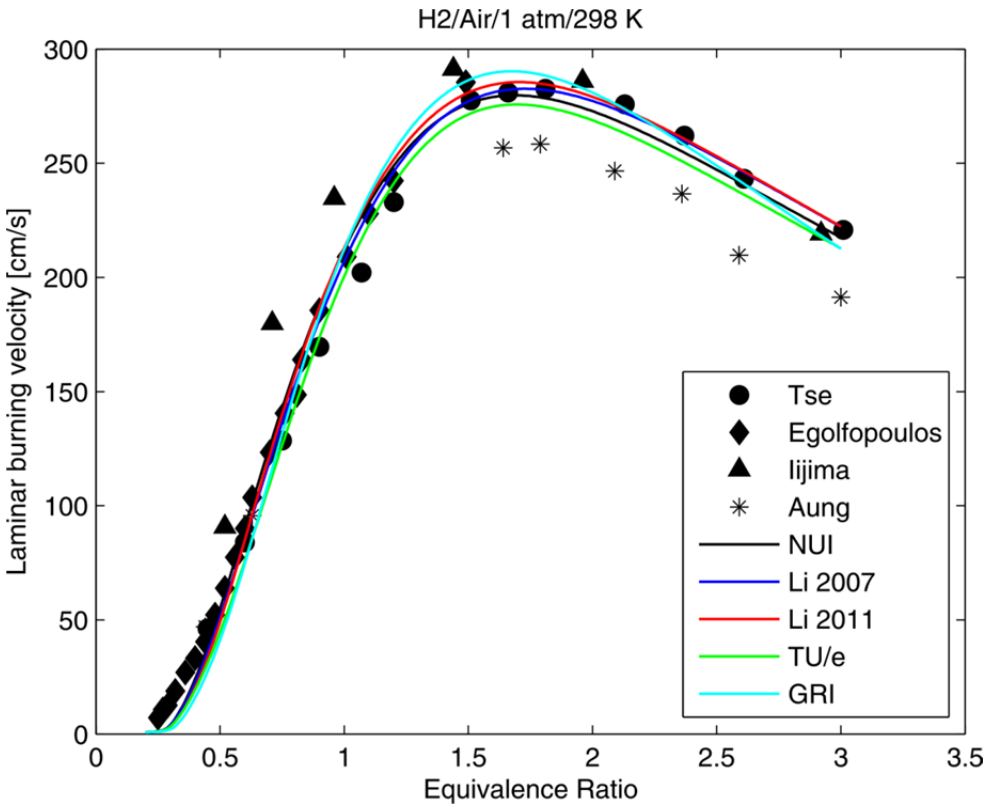

Figure 1: H_2/Air flame at 1 atm and 298 K, Experimental data [7-10]

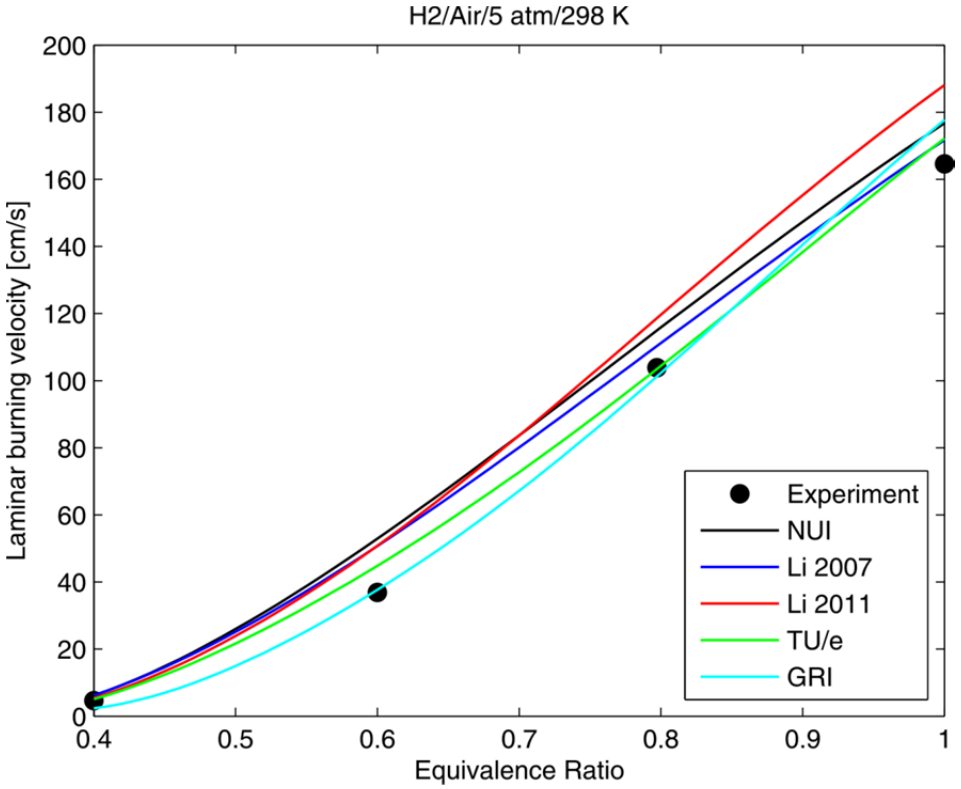

Figure 2: H_2/Air flame at 5 atm and 298 K, experiments from Kobayashi et al. [11]

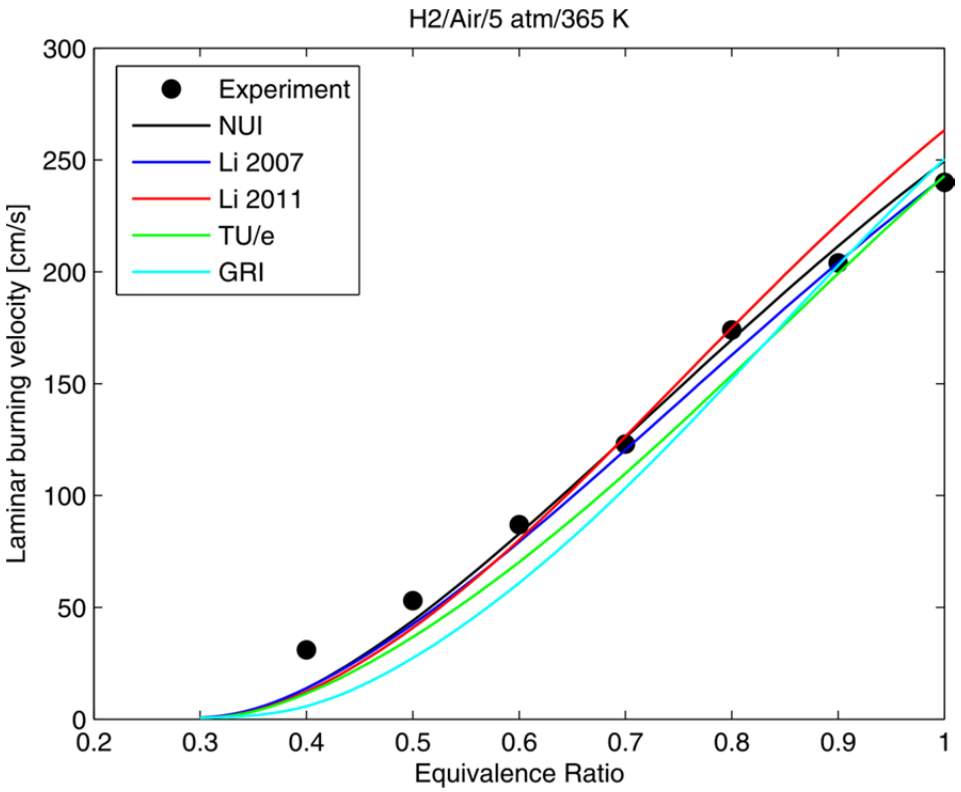

Figure 3: H_2/Air flame at 5 atm and 365 K, experiments from Bradley et al. [12]. The experimental uncertainties are very high (±15 cm/s)

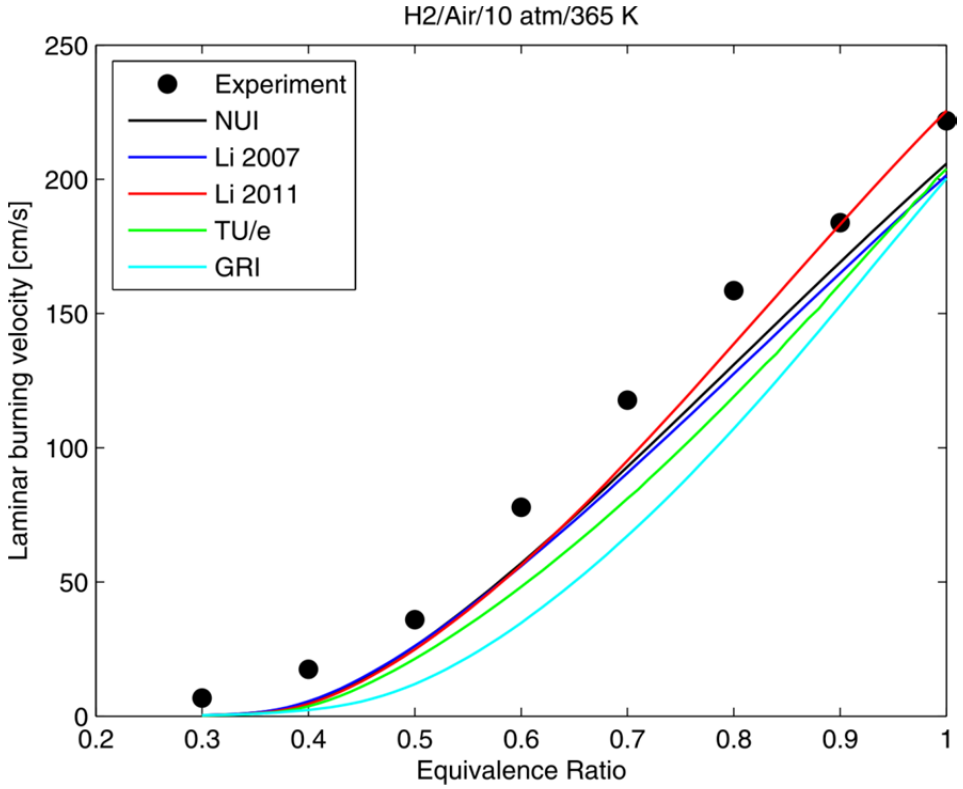

Figure 4: H_2/Air flame at 10 atm and 365 K, experiments from Bradley et al. [12]. The experimental uncertainties are very high (±30 cm/s)

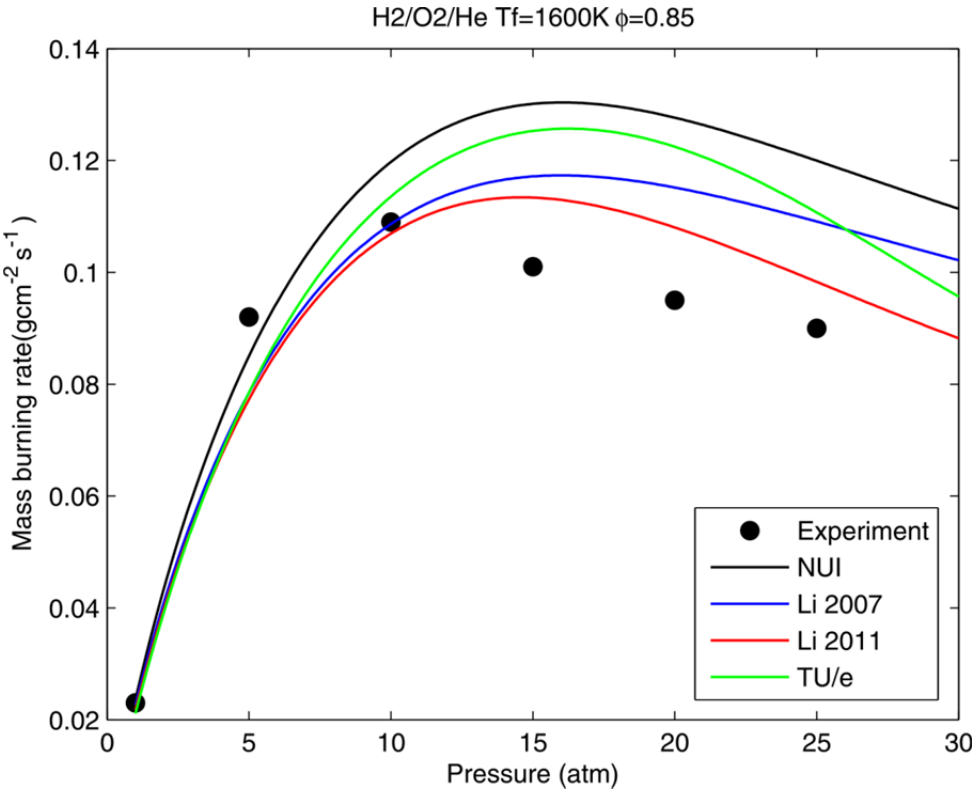

Figure 5: H_2/O_2/He flame at ϕ=0.85 and 298 K, experimental data from Burke et al. [13].

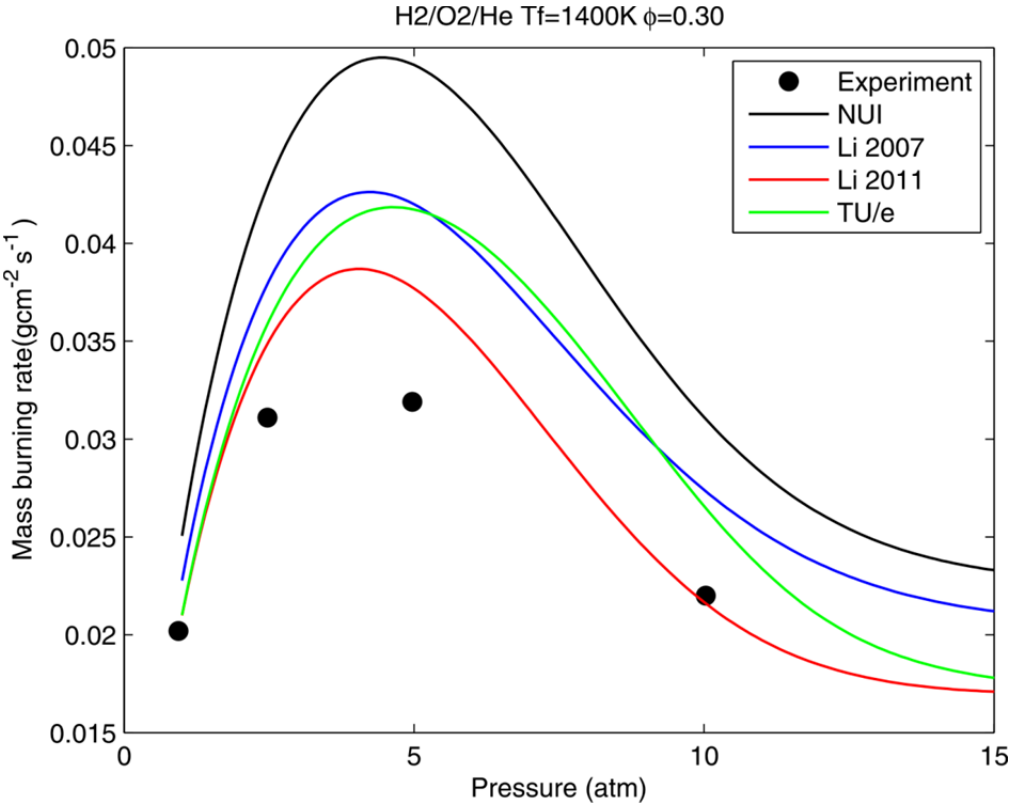

Figure 6: H_2/O_2/He flame at ϕ=0.3 and 298 K, experimental data from Burke et al. [13]

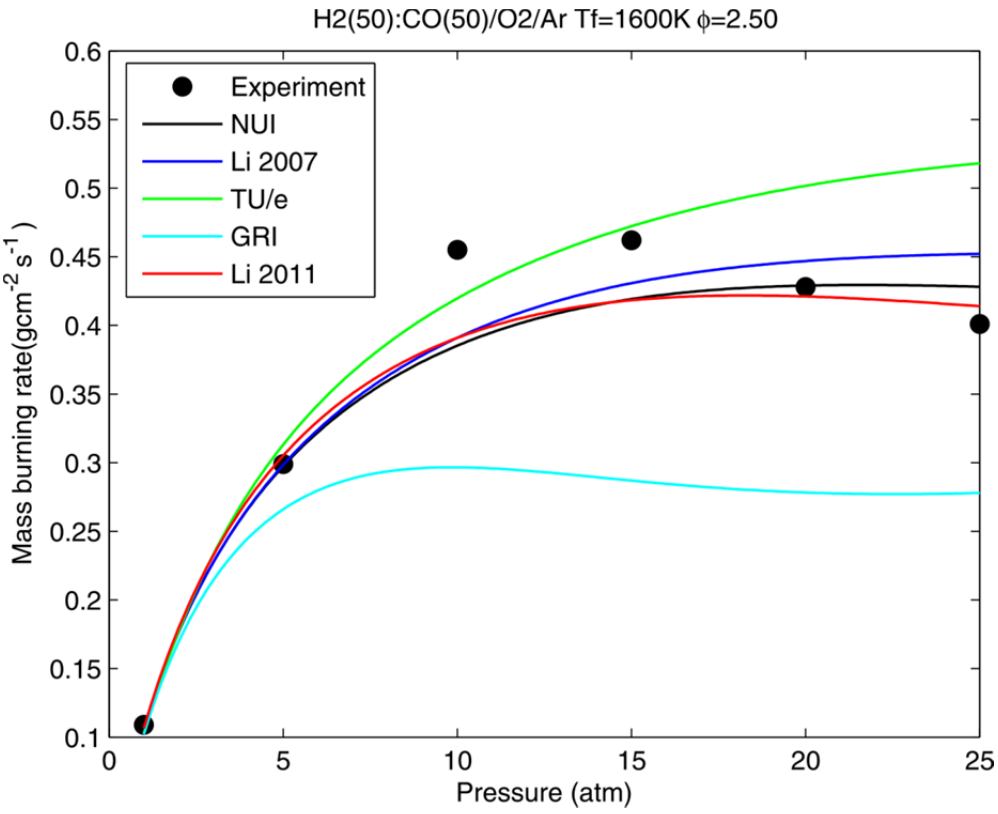

Figure 7: H_2/CO (50:50) and O_2/Ar flame at ϕ=2.5 and 298 K, experimental data from Burke et al. [13]

3.2 Experimental Results

This section outlines the measurements that have been made so far at TU Eindhoven using the "heat flux method [14"]. The fuel/oxidizer mixtures and operating conditions are listed in Table 1. Due to experimental problems (acoustic instabilities, non-uniform preheating) the uncertainty of the experimental results are relatively high (up to 4-6 cm/s) at this stage.

Table 1: Fuel/oxidizer mixtures and operating conditions

Fuel	CH_4	H_2/CO (50:50%)
Oxidizer	Air	Air
		O_2/N_2 (15:85%)
		O_2/N_2 (10:90%)
ϕ	0.8 – 1.4	0.6 – 1.0
T (K)	298	298
P (atm)	1.5 – 5	1.5 – 4

H_2/CO mixtures were studied in the heat flux system first at atmospheric conditions. Since the burner is enclosed in a high pressure cell, the flame is always exposed to a pressure higher that atmospheric. Hence, these results cannot be treated most accurate. However, it is indicative that flat flames can be stabilized on such burner. The velocities are of the order of 40-80 cm/s at atmospheric conditions when air is used as an oxidizer. As soon as the system was pressurized it was observed that the flame sweeped into an acoustical instability. To overcome this problem it was decided to dilute the oxidizer in order to obtain lower velocities (10-30 cm/s). Figure 8 depicts the flames at pressures up to 4 atm with diluted oxidizers – 10:90% and 15:85% O_2:N_2 (by volume) at equivalence ratio, φ = 0.7, 0.8, 1.0. In Figures 9-11 the experimental results have been compared with simulations using all mechanisms.

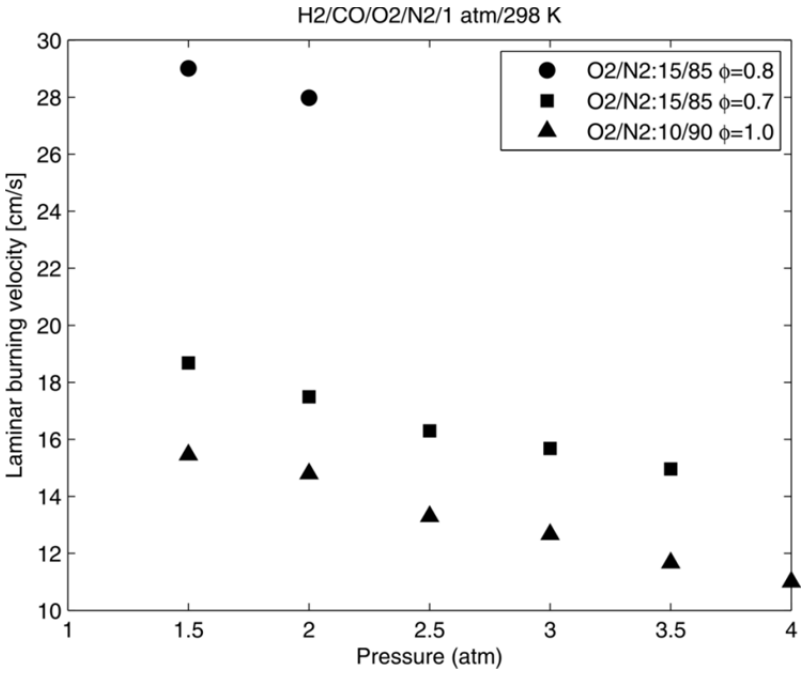

Figure 8: Results of high pressure H_2/CO (50:50) with diluted oxidizers

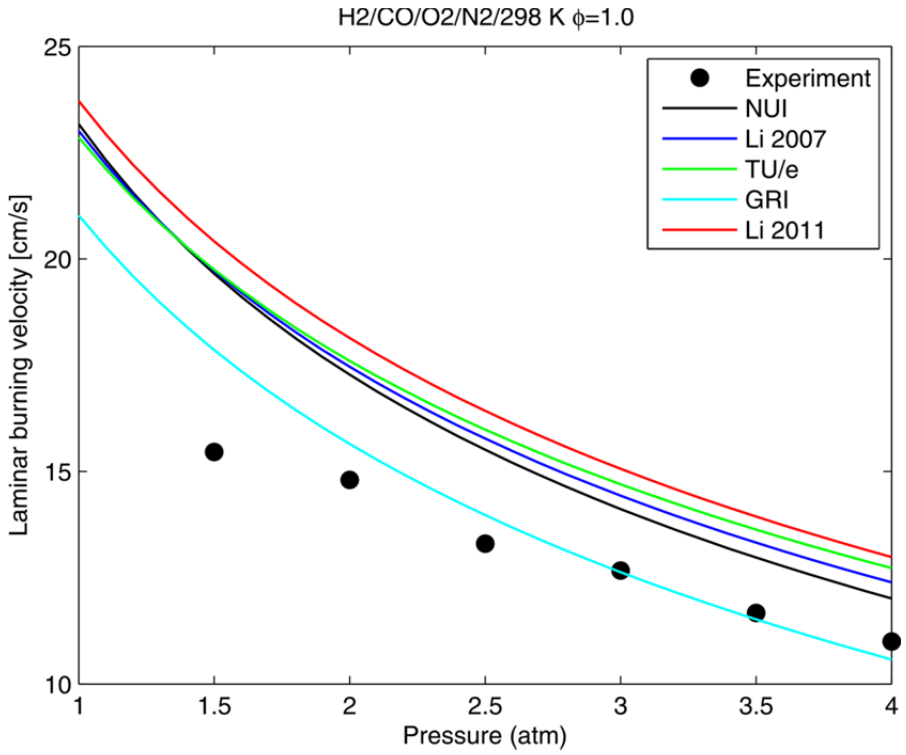

Figure 9: H_2/CO (50:50) with O_2/N_2 (10:90) at ϕ=1.0 at 298 K

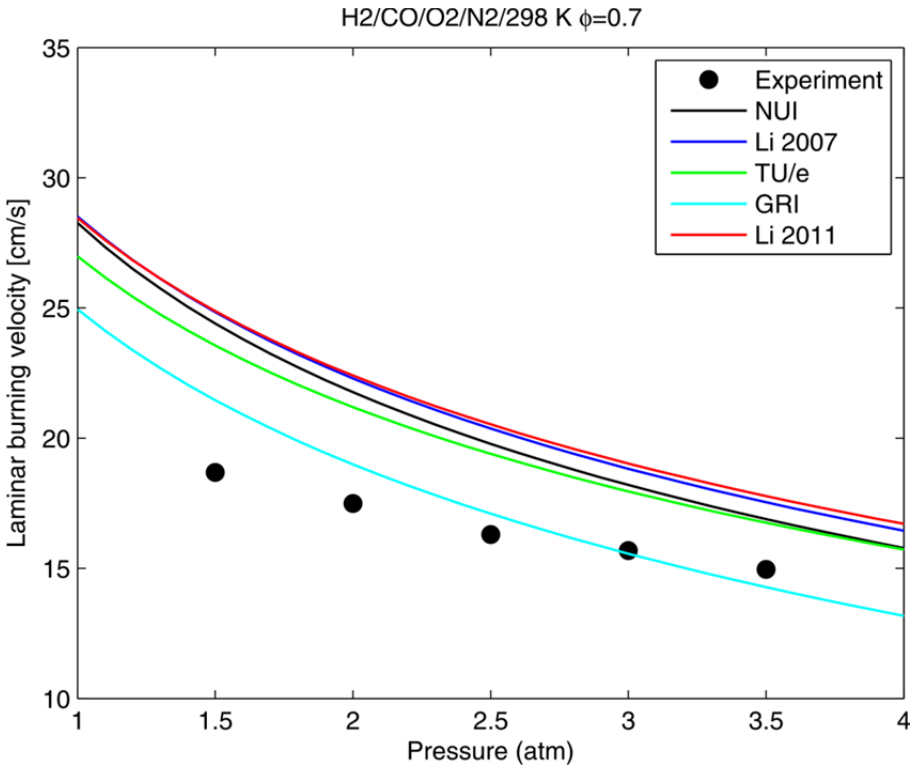

Figure 10: H_2/CO (50:50) with O_2/N_2 (15:85) at ϕ=0.7 at 298 K

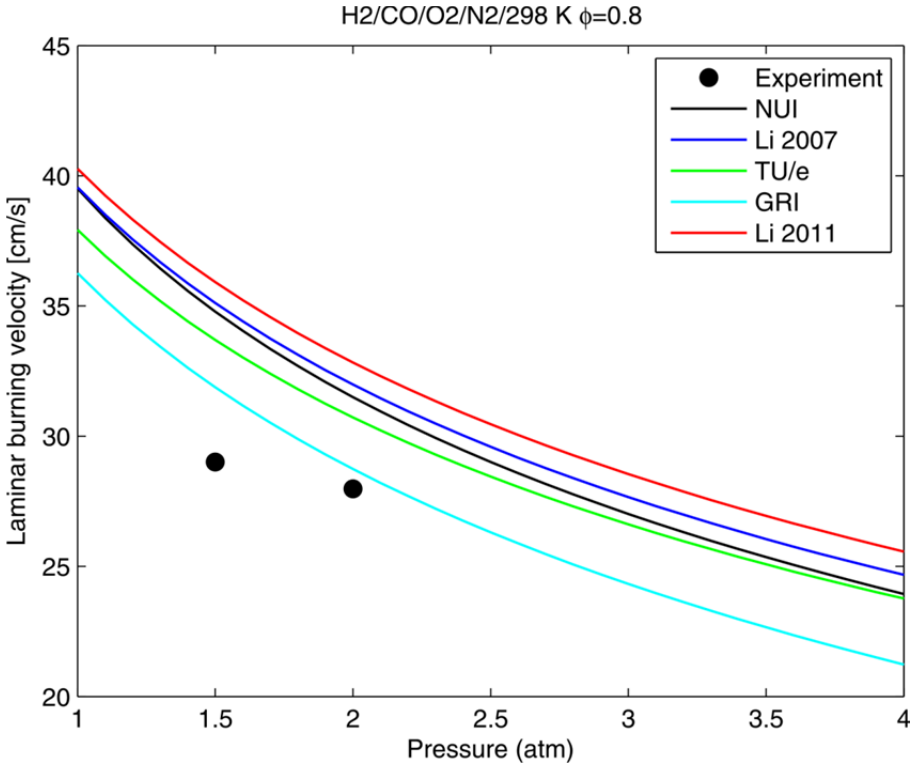

Figure 11: H_2/CO (50:50) with O_2/N_2 (15:85) at ϕ=0.8 at 298 K

Discussion

Laminar burning velocity of H_2/oxidizer flame is very sensitive to the reaction

$H+O_2=OH+O$.

From sensitivity analysis performed for this study and from literature the above equation has a negative coefficient. GRI 3.0 mechanism has the highest value of rate constant A (pre-exponential factor) among all the mechanisms compared in this study. Due to this fact, the GRI 3.0 mechanism shows lower burning velocities than others.

The comparison reveals that the simulation results using the mechanisms [1-4] all very similar, only the simulations with the GRI3.0 mechanism show significantly lower flame speed values. The agreement between the simulation results using the mechanisms [1-4] and the measured values is reasonable, especially if an underestimation of the experimental results of about 4-6 cm/s is taken into account. Future work aims at the generation of additional experimental data, e.g. at higher pressure, with a higher accuracy.

4. NO (TU/e)

An initial evaluation of the performance of the mechanisms [1-5] with respect to NO_X formation was performed by TU\e. The results of the simulations were compared with experimental data from literature [15]. The original kinetic schemes of the mechanisms [1-4] do not included any NO

chemistry. Therefore, in this study, the NO chemistry of the GRI3.0 mechanism was implemented in these mechanisms. NO can be formed via the following NO formation routes:

- Thermal NO
  - $O+N_2=N+NO$
  - $N+O_2=O+NO$
  - $N+OH=H+NO$
- Prompt NO
  - $CH+N_2=HCN+N$
  - $N+O_2=NO+O$
  - $HCN+OH=CN+H_2O$
- Others
  - $N_2+O=N_2O$
    - $N_2O+O=NO+NO$
    - $N_2O+H=NH+NO$
  - Via N_2H_3
    - $NNH \rightarrow N_2H_3 \rightarrow NH_3$
    - $NH_3 \rightarrow NH_2 \rightarrow NH \rightarrow N \rightarrow NO$
  - Via NNH
    - $N_2+H=NNH$
    - $NNH+O=NO+NH$

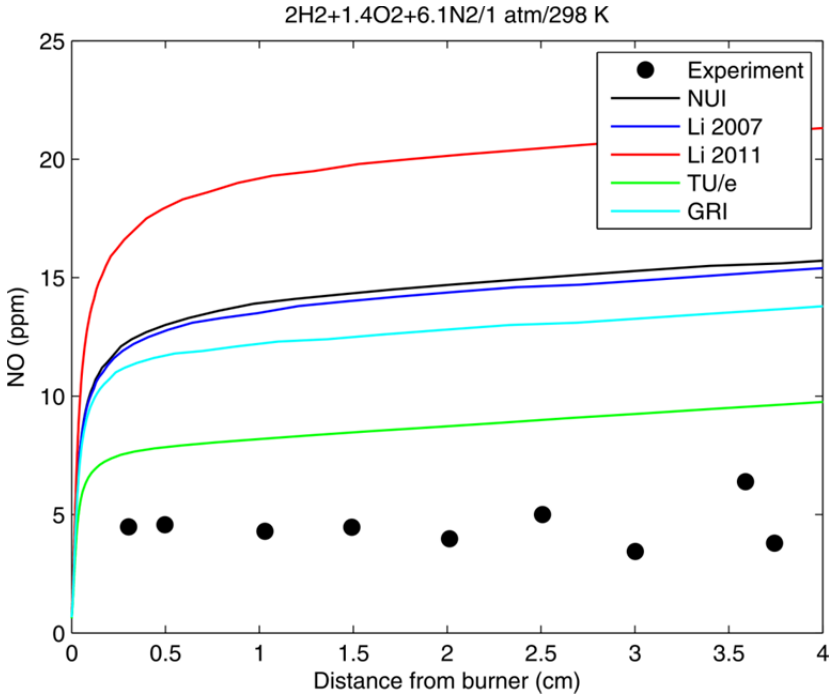

Figure 12: Comparison of axial NO profiles of a $H_2/O_2/N_2$ flame, O_2/N_2 (19%/81%), Φ = 0.71, 1 atm. Lines: simulation results of various mechanisms, Symbols: experimental data [15]

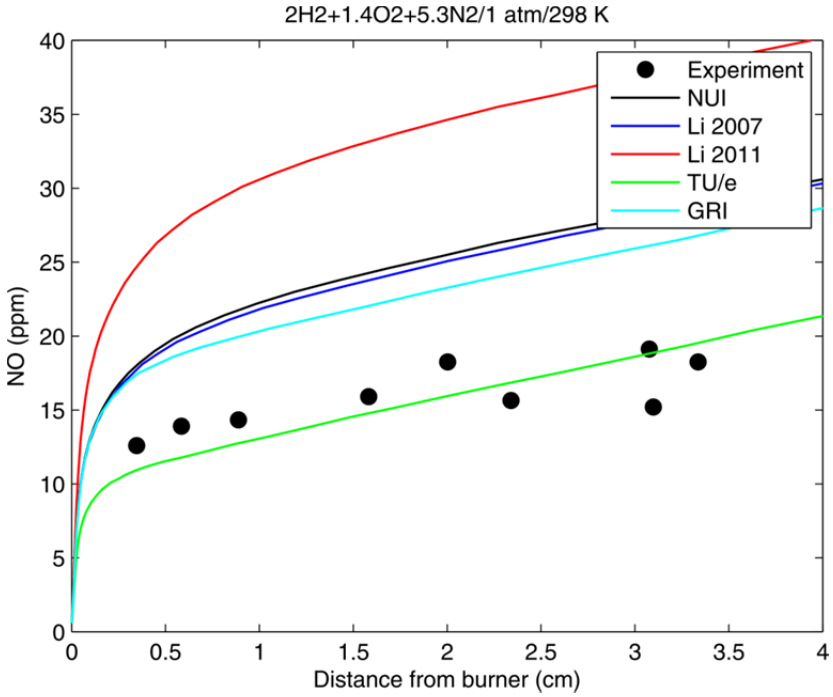

Figure 13: Comparison of axial NO profiles of a $H_2/O_2/N_2$ flame, O_2/N_2 (21%/79%), Φ = 0.71, 1 atm. Lines: simulation results of various mechanisms, Symbols: experimental data [15]

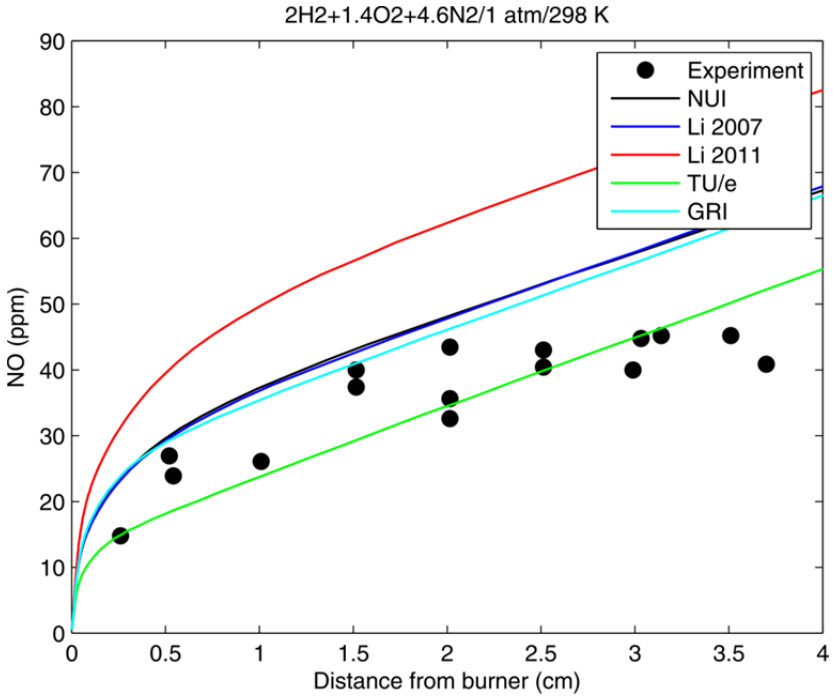

Figure 14: Comparison of axial NO profiles of a $H_2/O_2/N_2$ flame, O_2/N_2 (23%/77%), Φ = 0.71, 1 atm. Lines: simulation results of various mechanisms, Symbols: experimental data [15]

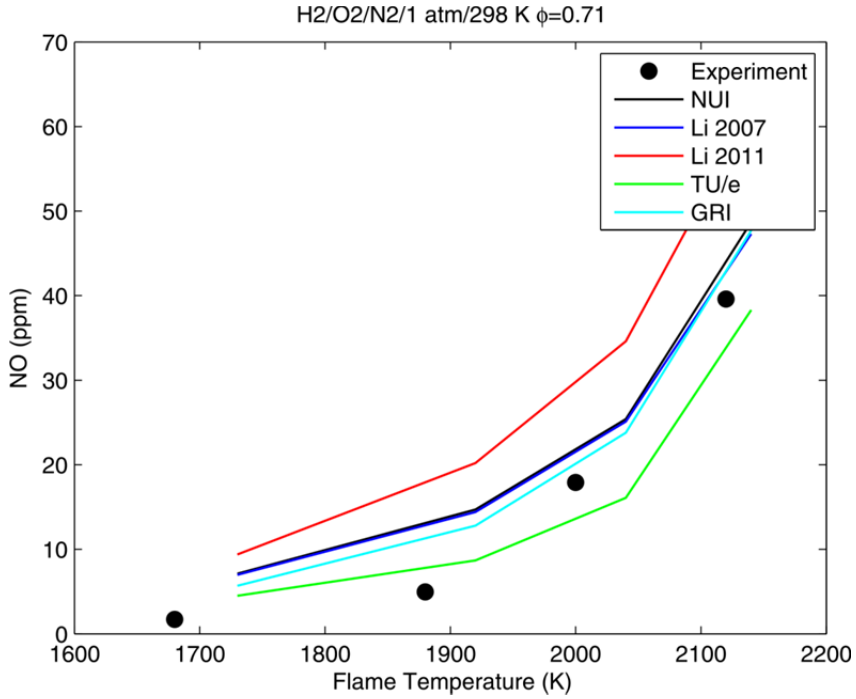

Figure 15: Measured (symbol [15]) and calculated (lines) NO concentration at an axial location 2 cm downstream of the flame front for a $H_2/O_2/N_2$ flame at different flame temperatures (oxidizer contents), Φ =0.71 and 1 atm

Discussion:

As shown in Figures 12-15, large differences in the simulated NO values can be observed. The results of the NUI Galway [1], the Li et al. 2007 [2] and the GRI 3.0 [5] mechanism are very similar. The values of the calculated NO using the TU/e mechanism [4] are always lower than for the others mechanisms. The highest NO values are calculated using the Li et al 2011 mechanism. With respect to NO concentrations, the following reactions play a major role:

$H+O_2=OH+O$	$H+O_2(+M)=HO_2(+M)$
$H+OH+M=H_2O+M$	$H_2+OH=H_2O+H$
$H_2O_2+OH=HO_2+H2O$	$N_2+O=NO+N$
$N_2O(+M)=N_2+O(+M)$	$N_2O+H=N_2+OH$
$N_2O+H=NH+NO$	$NNH+O=NH+NO$

Since in this study the same NO chemistry (from GRI3.0) was used in all mechanisms, the differences observed can only attributed to the rate constants of the H_2/CO sub mechanism. At higher flame temperatures (>1800 K), the thermal NO formation route plays the major role. However, at lower temperatures, other routes like N_2O and NNH become also important. In general, the concentration of the species like O_2, OH, O and H drive the NO formation. A more detailed sensitivity analysis will be performed in the next months in order to elucidate key reactions of the NO formation.

5. References

[1] NUI: newest update of the H2/CO mechanism of the NUI Galway (received 14/02/2012)

[2] Li et al. 2007: J. Li, Z. Zhao, A. Kazakov, M. Chaos, F.L. Dryer, J.J. Scire Jr, *Int. J. Chem. Kinet*. 39 (2007) 109-136, available at <http://www.princeton.edu/~combust/database/other.html>.

[3] Li et al. 2011: M.P. Burke, M. Chaos, F.L. Dryer, Y. Ju, and S.J. Klippenstein, "Comprehensive H2/O2 Kinetic Model for High-Pressure Combustion*", Int. J. Chem. Kin. (2011).* Available online Dec-06-2011. DOI:10.1002/kin.20603.

[4] TU/e. newest update of the H2/CO mechanism of the University of Eindhoven, M.Goswami, A.A.Konnov, R.J.M.Bastiaans,L.P.H de Goey, September 2011

[5] GRI 3.0 mechanism, Version 3.0 7/30/99, Smith, G.P., Golden, D.M., Frenklach, M., Moriarty, N.W., Eiteneer, B., Goldenberg, M., Bowman, C.T., Hanson, R.K., Song, S., Gardiner Jr., W.C., Lissianski, J., and Qin, Z. See http://www.me.berkeley.edu/gri_mech

[6] L.M.T. Somers, 'The simulation of flat flames with detailed and reduced chemical models', *PhD. Thesis*, Eindhoven University of Technology (1994).

[7] Egolfopoulos et al., *Proc Combust inst* (1990)

[8] Iijima et al. , *Combus Flame* (1986)

[9] Aung K.T., Hassan M.I., Faeth G.M., *Combus Flame*, 109: 1-24(1997).

[10] Tse S.D., Zhu D.L., Law C.K., *Proc. Combust Inst*., 28:1793-1800(2000).

[11] Kobayashi, H.,*Experimentalt hermal and fluid science* 26 (2002) 375-387.

[12] Bradley D., Lawes M., Liu K., Verhelst S., Woolley R., *Combus Flame* 149 (2007) 162-172.

[13] Burke M.P., Chaos M., Dryer F.L., Ju Y., *Combus. Flame* 157 (2010) 618-631.

[14] K.J. Bosschaart, 'Analysis of the Heat Flux Method for Measuring Burning Velocities', *PhD Thesis* , Department of Mechanical Engineering, Eindhoven University of Technology (2002).

[15] Homer J.B., Sutton M.M., *Combus Flame* 20:71-76(1973).